Sample Size Limitations for Frequency-Swept Free-Space Material Characterization

Richard J. Wylde*†, Graham S. Bell† and Axel Murk ‡
*School of Physics and Astronomy, St Andrews University, North Haugh, St Andrews, Fife, KY16 9SS, UK
†Thomas Keating Ltd, Station Mills, Billingshurst, West Sussex, RH14 9SH, UK
‡Institute of Applied Physics, University of Bern, Sidlerstrasse 5, CH-3012 Bern, Switzerland

***Abstract*—Modern THz devices depend on precise knowledge of material parameters, which, as the frequency coverage of VNA's pushes into the THz region, can be obtained from free-space measurements. However the interpretation of the results generally assumes an infinite plane wave propagating through the sample, whereas in practise a Gaussian beam-waist is typically located there. We discuss the error introduced by this, and the resulting limits on the size of the beam-waist and therefore the size of the material sample.**

I. Introduction

As the frequency coverage of high dynamic range Vector Network Analysers (VNA) pushes well into the THz region [1]–[3], high precision material measurements based upon free-space techniques become increasing possible. However the analyses of such measurements, giving complex permittivity and permeability, are generally based upon the assumption that the probing beam is infinite in extent. Given that samples are finite in size, this can not be the case and quasi-optical benches, such as the one we design and make, provide for a beam-waist at the sample position and the probing beams, formed by corrugated horns, are highly Gaussian in nature (up to 99.88% [4]).

How does this finite width affect the accuracy of the measurement? This is a practical problem, as it often drives both the size and expense of the sample which needs to be prepared, and the physical size and cost of the quasi-optical measurement bench.

Whereas previous work has considered the limitations on extracting permittivity and permeability parameters from measured data [5] and the error caused by the dispersion of a Gaussian beam on measurements taken at a single frequency [6], we consider a frequency swept measurement where the material parameters are to be determined by fitting the response as a function of frequency. Such a technique has been successfully applied, for example, to accurately characterize absorber materials [7] for the design of black-body calibration loads, and gyromagnetic material allowing the precise design of Faraday rotators [8]. In both cases knowledge of the permeability as well as the permittivity is required.

We present here a set of simulations based upon the angular-spectrum of plane waves **[REFERENCE]** (ASPW), which set out the errors to be expected in such measurements. We cover both the real (ε') and imaginary (ε'') parts of the permittivity.

II. The Model

A. Angular Spectrum of Plane Waves

A beam can be represented by an angular spectrum, $A(\theta, \phi)$, of plane waves. For two such beams, the coupling integral between them is then defined as

$$I_{ij} = \int_{\phi=0}^{2\pi} \int_{\theta=0}^{\pi/2} A_i^*(\theta, \phi) A_j(\theta, \phi) \sin\theta \, \mathrm{d}\theta \, \mathrm{d}\phi. \qquad (1)$$

A fundamental mode Gaussian beam, defining the beam-waist, w_0, as the $1/e$ amplitude radius, can be represented by

$$A_0(\theta, \phi) = \frac{1}{N} \, e^{-\left(\frac{\theta}{\theta_0}\right)^2} \qquad (2)$$

where the divergence angle is given by $\theta_0 = \frac{\lambda}{\pi w_0}$ and the normalization N is chosen so that the coupling integral of the beam with itself is unity, $I_{00} = 1$.

It is worth noting that the paraxial assumptions with underpin ASPW are the same as those for Fourier optics and Gaussian beam-mode optics, and the range of our angular spectra live within these constraints **(RJW TO EXPAND ON THIS)**.

B. Simulations

We decompose an input Gaussian beam into a discretized angular spectrum at the sample face, and propagate that set of plane waves though the sample by using the Fresnel equations to calculate the amplitude transmission coefficients for the electric field perpendicular to the plane of incidence, $t_\perp$ (TE polarization) and parallel to the plane of incidence, $t_\parallel$ (TM polarization). These components of each plane wave are $A(\theta, \phi) \cos\phi$ and $A(\theta, \phi) \sin\phi$ respectively, so that the amplitude of each plane wave, after passing through the sample, and resolved back into the original polarization, is

$$\begin{aligned} A_1(\theta, \phi) &= t_\perp(\theta, z, \nu) \, \cos^2(\phi) \, A_0(\theta, \phi) \\ &+ t_\parallel(\theta, z, \nu) \, \sin^2(\phi) \, A_0(\theta, \phi). \end{aligned} \qquad (3)$$

The complex coupling integral I_{21} is performed with a second Gaussian beam ($A_2(\theta, \phi) = A_0(\theta, \phi)$) to simulate measurement via the receiving corrugated feed horn, giving a predicted S_{21} transmission value in both amplitude and phase. The input parameters for the simulation are the frequency, material thickness, divergence angle, permittivity (real part ε' and imaginary part ε'') and permeability of the sample.

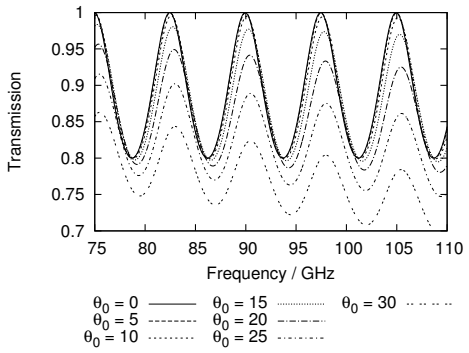

Fig. 1. Example simulated transmission values for 7 different values of θ_0, with $\varepsilon = 4$ and $d = 10$.

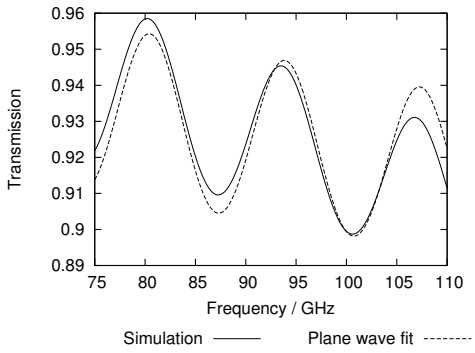

Fig. 2. Example simulation results and the corresponding fitted normal incidence plane wave transmission. The simulation input parameters were $\varepsilon' = 2$, $\varepsilon'' = 0$, a sample width of $d = 8\,\text{mm}$ and a divergence of $\theta_0 = 20°$, and the fitted dielectric parameters were $\varepsilon' = 1.949$ and $\varepsilon'' = 0.009$.

III. Results

A. General Behaviour

Keeping all but the frequency fixed, transmission plots against frequency — which simulate experimental results from a VNA measurement — can be produced. Fig. 1 illustrates the effect of the Gaussian beam on a lossless sample: as the divergence angle is increased, the resonant transmission peaks become further spread out, mimicking a decrease in refractive index. In addition the power retained in the fundamental Gaussian mode decreases, making the material appear lossy.

B. Error in Extracted Parameters

The simulated transmission plots were then fitted to a model assuming just a normal incidence plane wave, making use of both phase and amplitude information. An example of such a fit is given in Fig. 2. The difference between the original and fitted sets of complex material parameters then provides an estimate of the systematic error which would arise in extracting the material parameters from measured data.

We have run this procedure over a range of material parameters, sample thickness and divergence angles, giving the results presented in Fig. 3 and 4, in each case calculating the error in the extracted parameters. From these results we have plotted in Fig. 5 the divergence angle at which there is 1% error in the real part of the permittivity and 0.25% error in the imaginary part. There is some ripple at the low thickness end of the graphs where there is ambiguity in the fitting process due to the small number of wavelengths in the sample. Away from this, however, the results appear largely independent of the thickness, d, and approximately linear in ε', where we find the relation for 1% error in ε' to be approximately $\theta_0 \sim 7.76(1 + 0.284\varepsilon')$. Therefore the minimum beam waist for this error level is given by $w_0 \sim \frac{2.4}{1+0.28\varepsilon'}\lambda$.

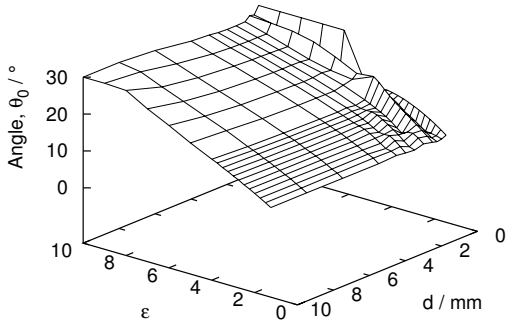

(a) 1% error in ε'.

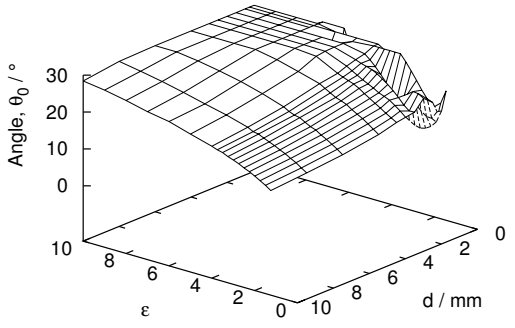

(b) 0.25% error in ε'' as a fraction of $|\varepsilon|$.

Fig. 5. Plots showing the maximum divergence angle permissible to achieve the specified accuracy.

IV. Conclusion

Given the need to have low edge tapers at the sample edges, we recommend a very minimum sample diameter of $3w_0$, giving a 20 dB edge taper, or ideally $4w_0$ or greater (≥ 35 dB edge taper). So taking 1% as an allowable error, the allowable sample sizes are smaller than we might have expected. Given the systematic nature of the errors introduced by finite beam sizes, it would be possible to use this type of analysis to apply a correction for small sample measurements.

Acknowledgement

The authors would like to thank Axel Murk of the Institute of Applied Physics, University of Bern for making available a MATLAB function to calculate the complex transmission and reflection parameters for a system of layered media.

References

[1] Agilent Technologies PNA network analyzers. [Online]. Available: http://www.home.agilent.com/agilent/product.jspx?nid=-536902643.0.00

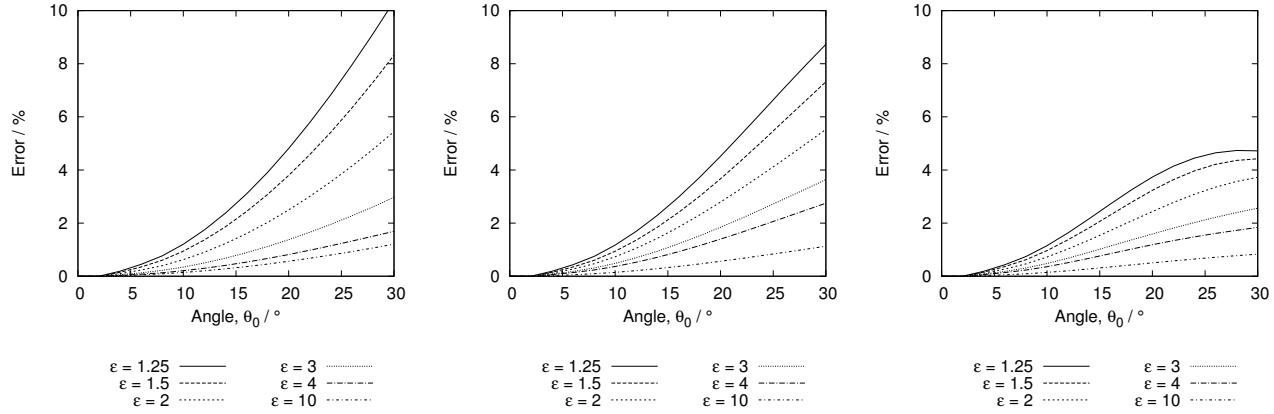

(a) $d = 1\,\mathrm{mm}$ (b) $d = 4\,\mathrm{mm}$ (c) $d = 10\,\mathrm{mm}$

Fig. 3. Error in the real part of the permittivity for lossless samples ($\varepsilon'' = 0$).

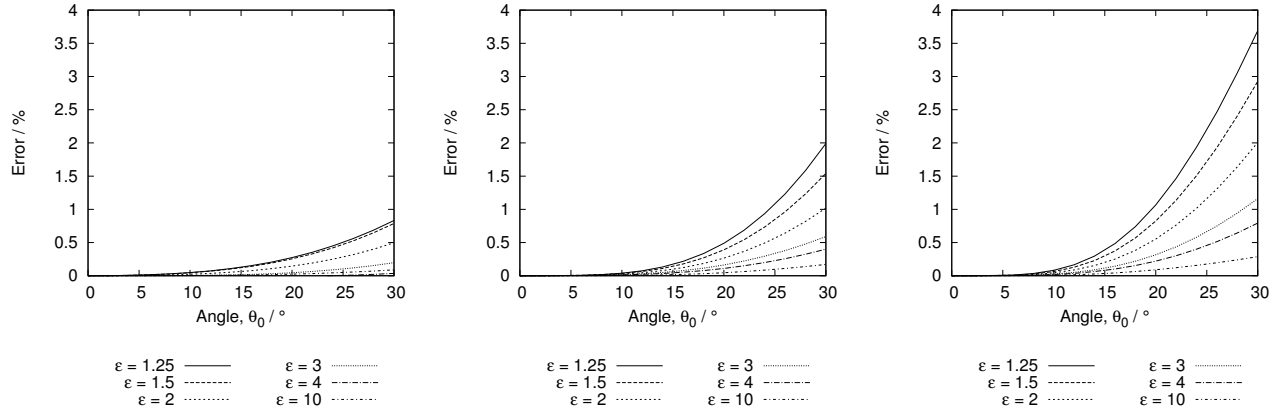

(a) $d = 1\,\mathrm{mm}$ (b) $d = 4\,\mathrm{mm}$ (c) $d = 10\,\mathrm{mm}$

Fig. 4. Error in the imaginary part of the permittivity for lossless samples ($\varepsilon'' = 0$).

[2] Rohde & Schwarz ZVA vector network analyzers. [Online]. Available: http://www2.rohde-schwarz.com/product/ZVA.html

[3] P. Goy. The AB Millimetre website. [Online]. Available: http://www.abmillimetre.com/

[4] P. A. Cruickshank, D. R. Bolton, D. A. Robertson, R. J. Wylde, and G. M. Smith, "Reducing standing waves in quasi-optical systems by optimal feedhorn design," in *Joint 32nd Int. Conf. Infrared and Millimeter Waves, and 15th Int. Conf. on Terahertz Electronics*, vol. 2, Cardiff, Sep. 2007, pp. 941–942.

[5] D. Sjöberg and C. Larsson, "Cramér-Rao bounds for determination of permittivity and permeability in slabs," *IEEE Trans. Microw. Theory Tech.*, vol. 59, no. 11, pp. 2970–2977, Nov. 2011.

[6] L. E. R. Petersson and G. S. Smith, "An estimate of the error caused by the plane-wave approximation in free-space dielectric measurement systems," *IEEE Trans. Antennas Propag.*, vol. 50, no. 6, pp. 878–887, Aug. 2002.

[7] I. Zivkovic and A. Murk, "Characterization of magnetically loaded microwave absorbers," *Progress In Electromagnetics Research B*, vol. 33, pp. 277–289, 2011.

[8] D. H. Martin and R. J. Wylde, "Wideband circulators for use at frequencies above 100 GHz to beyond 350 GHz," *IEEE Trans. Microw. Theory Tech.*, vol. 57, no. 1, pp. 99–108, Jan. 2009.